Measurement of the W boson production charge asymmetry in $p\bar{p} \to W + X \to e\nu + X$ events at $\sqrt{s} = 1.96$ TeV

V.M. Abazov, F. Badaud, Ph. Gris, G. Bernardi, D. Brown, Y. Enari, J. Lellouch, D. Li, L. Zivkovic, S. Greder, et al.

▶ **To cite this version:**

V.M. Abazov, F. Badaud, Ph. Gris, G. Bernardi, D. Brown, et al.. Measurement of the W boson production charge asymmetry in $p\bar{p} \to W + X \to e\nu + X$ events at $\sqrt{s} = 1.96$ TeV. Physical Review Letters, 2014, 112, pp.151803. 10.1103/PhysRevLett.112.151803 . in2p3-00916934

HAL Id: in2p3-00916934
https://hal.in2p3.fr/in2p3-00916934

Submitted on 7 Sep 2023

HAL is a multi-disciplinary open access archive for the deposit and dissemination of scientific research documents, whether they are published or not. The documents may come from teaching and research institutions in France or abroad, or from public or private research centers.

L'archive ouverte pluridisciplinaire **HAL**, est destinée au dépôt et à la diffusion de documents scientifiques de niveau recherche, publiés ou non, émanant des établissements d'enseignement et de recherche français ou étrangers, des laboratoires publics ou privés.

FERMILAB-PUB-13-567-E

arXiv:1312.2895v4 [hep-ex] 10 Dec 2014

Erratum: Measurement of the W boson production charge asymmetry in $p\bar{p} \to W + X \to e\nu + X$ events at $\sqrt{s} = 1.96$ TeV

V.M. Abazov,[31] B. Abbott,[66] B.S. Acharya,[25] M. Adams,[45] T. Adams,[43] J.P. Agnew,[40] G.D. Alexeev,[31] G. Alkhazov,[35] A. Alton[a],[55] A. Askew,[43] S. Atkins,[53] K. Augsten,[7] C. Avila,[5] F. Badaud,[10] L. Bagby,[44] B. Baldin,[44] D.V. Bandurin,[72] S. Banerjee,[25] E. Barberis,[54] P. Baringer,[52] J.F. Bartlett,[44] U. Bassler,[15] V. Bazterra,[45] A. Bean,[52] M. Begalli,[2] L. Bellantoni,[44] S.B. Beri,[23] G. Bernardi,[14] R. Bernhard,[19] I. Bertram,[38] M. Besançon,[15] R. Beuselinck,[39] P.C. Bhat,[44] S. Bhatia,[57] V. Bhatnagar,[23] G. Blazey,[46] S. Blessing,[43] K. Bloom,[58] A. Boehnlein,[44] D. Boline,[63] E.E. Boos,[33] G. Borissov,[38] A. Brandt,[69] O. Brandt,[20] R. Brock,[56] A. Bross,[44] D. Brown,[14] X.B. Bu,[44] M. Buehler,[44] V. Buescher,[21] V. Bunichev,[33] S. Burdin[b],[38] C.P. Buszello,[37] E. Camacho-Pérez,[28] B.C.K. Casey,[44] H. Castilla-Valdez,[28] S. Caughron,[56] S. Chakrabarti,[63] K.M. Chan,[50] A. Chandra,[71] E. Chapon,[15] G. Chen,[52] S.W. Cho,[27] S. Choi,[27] B. Choudhary,[24] S. Cihangir,[44] D. Claes,[58] J. Clutter,[52] M. Cooke[k],[44] W.E. Cooper,[44] M. Corcoran,[71] F. Couderc,[15] M.-C. Cousinou,[12] D. Cutts,[68] A. Das,[41] G. Davies,[39] S.J. de Jong,[29,30] E. De La Cruz-Burelo,[28] F. Déliot,[15] R. Demina,[62] D. Denisov,[44] S.P. Denisov,[34] S. Desai,[44] C. Deterre[c],[20] K. DeVaughan,[58] H.T. Diehl,[44] M. Diesburg,[44] P.F. Ding,[40] A. Dominguez,[58] A. Dubey,[24] L.V. Dudko,[33] A. Duperrin,[12] S. Dutt,[23] M. Eads,[46] D. Edmunds,[56] J. Ellison,[42] V.D. Elvira,[44] Y. Enari,[14] H. Evans,[48] V.N. Evdokimov,[34] L. Feng,[46] T. Ferbel,[62] F. Fiedler,[21] F. Filthaut,[29,30] W. Fisher,[56] H.E. Fisk,[44] M. Fortner,[46] H. Fox,[38] S. Fuess,[44] P.H. Garbincius,[44] A. Garcia-Bellido,[62] J.A. García-González,[28] V. Gavrilov,[32] W. Geng,[12,56] C.E. Gerber,[45] Y. Gershtein,[59] G. Ginther,[44,62] G. Golovanov,[31] P.D. Grannis,[63] S. Greder,[16] H. Greenlee,[44] G. Grenier,[17] Ph. Gris,[10] J.-F. Grivaz,[13] A. Grohsjean[c],[15] S. Grünendahl,[44] M.W. Grünewald,[26] T. Guillemin,[13] G. Gutierrez,[44] P. Gutierrez,[66] J. Haley,[67] L. Han,[4] K. Harder,[40] A. Harel,[62] J.M. Hauptman,[51] J. Hays,[39] T. Head,[40] T. Hebbeker,[18] D. Hedin,[46] H. Hegab,[67] A.P. Heinson,[42] U. Heintz,[68] C. Hensel,[20] I. Heredia-De La Cruz[d],[28] K. Herner,[44] G. Hesketh[f],[40] M.D. Hildreth,[50] R. Hirosky,[72] T. Hoang,[43] J.D. Hobbs,[63] B. Hoeneisen,[9] J. Hogan,[71] M. Hohlfeld,[21] J.L. Holzbauer,[57] I. Howley,[69] Z. Hubacek,[7,15] V. Hynek,[7] I. Iashvili,[61] Y. Ilchenko,[70] R. Illingworth,[44] A.S. Ito,[44] S. Jabeen,[68] M. Jaffré,[13] A. Jayasinghe,[66] M.S. Jeong,[27] R. Jesik,[39] P. Jiang,[4] K. Johns,[41] E. Johnson,[56] M. Johnson,[44] A. Jonckheere,[44] P. Jonsson,[39] J. Joshi,[42] A.W. Jung,[44] A. Juste,[36] E. Kajfasz,[12] D. Karmanov,[33] I. Katsanos,[58] R. Kehoe,[70] S. Kermiche,[12] N. Khalatyan,[44] A. Khanov,[67] A. Kharchilava,[61] Y.N. Kharzheev,[31] I. Kiselevich,[32] J.M. Kohli,[23] A.V. Kozelov,[34] J. Kraus,[57] A. Kumar,[61] A. Kupco,[8] T. Kurča,[17] V.A. Kuzmin,[33] S. Lammers,[48] P. Lebrun,[17] H.S. Lee,[27] S.W. Lee,[51] W.M. Lee,[44] X. Lei,[41] J. Lellouch,[14] D. Li,[14] H. Li,[72] L. Li,[42] Q.Z. Li,[44] J.K. Lim,[27] D. Lincoln,[44] J. Linnemann,[56] V.V. Lipaev,[34] R. Lipton,[44] H. Liu,[70] Y. Liu,[4] A. Lobodenko,[35] M. Lokajicek,[8] R. Lopes de Sa,[63] R. Luna-Garcia[g],[28] A.L. Lyon,[44] A.K.A. Maciel,[1] R. Madar,[19] R. Magaña-Villalba,[28] S. Malik,[58] V.L. Malyshev,[31] J. Mansour,[20] J. Martínez-Ortega,[28] R. McCarthy,[63] C.L. McGivern,[40] M.M. Meijer,[29,30] A. Melnitchouk,[44] D. Menezes,[46] P.G. Mercadante,[3] M. Merkin,[33] A. Meyer,[18] J. Meyer[i],[20] F. Miconi,[16] N.K. Mondal,[25] M. Mulhearn,[72] E. Nagy,[12] M. Narain,[68] R. Nayyar,[41] H.A. Neal,[55] J.P. Negret,[5] P. Neustroev,[35] H.T. Nguyen,[72] T. Nunnemann,[22] J. Orduna,[71] N. Osman,[12] J. Osta,[50] A. Pal,[69] N. Parashar,[49] V. Parihar,[68] S.K. Park,[27] R. Partridge[e],[68] N. Parua,[48] A. Patwa[j],[64] B. Penning,[44] M. Perfilov,[33] Y. Peters,[40] K. Petridis,[40] G. Petrillo,[62] P. Pétroff,[13] M.-A. Pleier,[64] V.M. Podstavkov,[44] A.V. Popov,[34] M. Prewitt,[71] D. Price,[40] N. Prokopenko,[34] J. Qian,[55] A. Quadt,[20] B. Quinn,[57] P.N. Ratoff,[38] I. Razumov,[34] I. Ripp-Baudot,[16] F. Rizatdinova,[67] M. Rominsky,[44] A. Ross,[38] C. Royon,[15] P. Rubinov,[44] R. Ruchti,[50] G. Sajot,[11] A. Sánchez-Hernández,[28] M.P. Sanders,[22] A.S. Santos[h],[1] G. Savage,[44] L. Sawyer,[53] T. Scanlon,[39] R.D. Schamberger,[63] Y. Scheglov,[35] H. Schellman,[47] C. Schwanenberger,[40] R. Schwienhorst,[56] J. Sekaric,[52] H. Severini,[66] E. Shabalina,[20] V. Shary,[15] S. Shaw,[56] A.A. Shchukin,[34] V. Simak,[7] P. Skubic,[66] P. Slattery,[62] D. Smirnov,[50] G.R. Snow,[58] J. Snow,[65] S. Snyder,[64] S. Söldner-Rembold,[40] L. Sonnenschein,[18] K. Soustruznik,[6] J. Stark,[11] D.A. Stoyanova,[34] M. Strauss,[66] L. Suter,[40] P. Svoisky,[66] M. Titov,[15] V.V. Tokmenin,[31] Y.-T. Tsai,[62] D. Tsybychev,[63] B. Tuchming,[15] C. Tully,[60] L. Uvarov,[35] S. Uvarov,[35] S. Uzunyan,[46] R. Van Kooten,[48] W.M. van Leeuwen,[29] N. Varelas,[45] E.W. Varnes,[41] I.A. Vasilyev,[34] A.Y. Verkheev,[31] L.S. Vertogradov,[31] M. Verzocchi,[44] M. Vesterinen,[40] D. Vilanova,[15] P. Vokac,[7] H.D. Wahl,[43] M.H.L.S. Wang,[44] J. Warchol,[50] G. Watts,[73] M. Wayne,[50] J. Weichert,[21] L. Welty-Rieger,[47]

M.R.J. Williams,[48] G.W. Wilson,[52] M. Wobisch,[53] D.R. Wood,[54] T.R. Wyatt,[40] Y. Xie,[44] R. Yamada,[44] S. Yang,[4] T. Yasuda,[44] Y.A. Yatsunenko,[31] W. Ye,[63] Z. Ye,[44] H. Yin,[44] K. Yip,[64] S.W. Youn,[44] J.M. Yu,[55] J. Zennamo,[61] T.G. Zhao,[40] B. Zhou,[55] J. Zhu,[55] M. Zielinski,[62] D. Zieminska,[48] and L. Zivkovic[14]

(The D0 Collaboration*)

[1]*LAFEX, Centro Brasileiro de Pesquisas Físicas, Rio de Janeiro, Brazil*
[2]*Universidade do Estado do Rio de Janeiro, Rio de Janeiro, Brazil*
[3]*Universidade Federal do ABC, Santo André, Brazil*
[4]*University of Science and Technology of China, Hefei, People's Republic of China*
[5]*Universidad de los Andes, Bogotá, Colombia*
[6]*Charles University, Faculty of Mathematics and Physics, Center for Particle Physics, Prague, Czech Republic*
[7]*Czech Technical University in Prague, Prague, Czech Republic*
[8]*Institute of Physics, Academy of Sciences of the Czech Republic, Prague, Czech Republic*
[9]*Universidad San Francisco de Quito, Quito, Ecuador*
[10]*LPC, Université Blaise Pascal, CNRS/IN2P3, Clermont, France*
[11]*LPSC, Université Joseph Fourier Grenoble 1, CNRS/IN2P3, Institut National Polytechnique de Grenoble, Grenoble, France*
[12]*CPPM, Aix-Marseille Université, CNRS/IN2P3, Marseille, France*
[13]*LAL, Université Paris-Sud, CNRS/IN2P3, Orsay, France*
[14]*LPNHE, Universités Paris VI and VII, CNRS/IN2P3, Paris, France*
[15]*CEA, Irfu, SPP, Saclay, France*
[16]*IPHC, Université de Strasbourg, CNRS/IN2P3, Strasbourg, France*
[17]*IPNL, Université Lyon 1, CNRS/IN2P3, Villeurbanne, France and Université de Lyon, Lyon, France*
[18]*III. Physikalisches Institut A, RWTH Aachen University, Aachen, Germany*
[19]*Physikalisches Institut, Universität Freiburg, Freiburg, Germany*
[20]*II. Physikalisches Institut, Georg-August-Universität Göttingen, Göttingen, Germany*
[21]*Institut für Physik, Universität Mainz, Mainz, Germany*
[22]*Ludwig-Maximilians-Universität München, München, Germany*
[23]*Panjab University, Chandigarh, India*
[24]*Delhi University, Delhi, India*
[25]*Tata Institute of Fundamental Research, Mumbai, India*
[26]*University College Dublin, Dublin, Ireland*
[27]*Korea Detector Laboratory, Korea University, Seoul, Korea*
[28]*CINVESTAV, Mexico City, Mexico*
[29]*Nikhef, Science Park, Amsterdam, the Netherlands*
[30]*Radboud University Nijmegen, Nijmegen, the Netherlands*
[31]*Joint Institute for Nuclear Research, Dubna, Russia*
[32]*Institute for Theoretical and Experimental Physics, Moscow, Russia*
[33]*Moscow State University, Moscow, Russia*
[34]*Institute for High Energy Physics, Protvino, Russia*
[35]*Petersburg Nuclear Physics Institute, St. Petersburg, Russia*
[36]*Institució Catalana de Recerca i Estudis Avançats (ICREA) and Institut de Física d'Altes Energies (IFAE), Barcelona, Spain*
[37]*Uppsala University, Uppsala, Sweden*
[38]*Lancaster University, Lancaster LA1 4YB, United Kingdom*
[39]*Imperial College London, London SW7 2AZ, United Kingdom*
[40]*The University of Manchester, Manchester M13 9PL, United Kingdom*
[41]*University of Arizona, Tucson, Arizona 85721, USA*
[42]*University of California Riverside, Riverside, California 92521, USA*
[43]*Florida State University, Tallahassee, Florida 32306, USA*
[44]*Fermi National Accelerator Laboratory, Batavia, Illinois 60510, USA*
[45]*University of Illinois at Chicago, Chicago, Illinois 60607, USA*
[46]*Northern Illinois University, DeKalb, Illinois 60115, USA*
[47]*Northwestern University, Evanston, Illinois 60208, USA*
[48]*Indiana University, Bloomington, Indiana 47405, USA*
[49]*Purdue University Calumet, Hammond, Indiana 46323, USA*
[50]*University of Notre Dame, Notre Dame, Indiana 46556, USA*
[51]*Iowa State University, Ames, Iowa 50011, USA*
[52]*University of Kansas, Lawrence, Kansas 66045, USA*
[53]*Louisiana Tech University, Ruston, Louisiana 71272, USA*
[54]*Northeastern University, Boston, Massachusetts 02115, USA*
[55]*University of Michigan, Ann Arbor, Michigan 48109, USA*
[56]*Michigan State University, East Lansing, Michigan 48824, USA*

[57] University of Mississippi, University, Mississippi 38677, USA
[58] University of Nebraska, Lincoln, Nebraska 68588, USA
[59] Rutgers University, Piscataway, New Jersey 08855, USA
[60] Princeton University, Princeton, New Jersey 08544, USA
[61] State University of New York, Buffalo, New York 14260, USA
[62] University of Rochester, Rochester, New York 14627, USA
[63] State University of New York, Stony Brook, New York 11794, USA
[64] Brookhaven National Laboratory, Upton, New York 11973, USA
[65] Langston University, Langston, Oklahoma 73050, USA
[66] University of Oklahoma, Norman, Oklahoma 73019, USA
[67] Oklahoma State University, Stillwater, Oklahoma 74078, USA
[68] Brown University, Providence, Rhode Island 02912, USA
[69] University of Texas, Arlington, Texas 76019, USA
[70] Southern Methodist University, Dallas, Texas 75275, USA
[71] Rice University, Houston, Texas 77005, USA
[72] University of Virginia, Charlottesville, Virginia 22904, USA
[73] University of Washington, Seattle, Washington 98195, USA

(Dated: December 10, 2013)

PACS numbers: 13.38.Be, 13.85.Qk, 14.60.Cd, 14.70.Fm

The measurement of the W boson production charge asymmetry published in our recent Letter [1] employed a correction $K^{\pm}_{\rm eff}$ to take into account the relative efficiency difference between electrons and positrons. Based on a recent study [2], we realized that the determination of $K^{\pm}_{\rm eff}$ was incorrect. Instead of taking the ratio of the positron to electron efficiencies, we took the ratio of the numbers of reconstructed positrons to electrons. In addition, we had not taken into account the solenoid polarity when determining $K^{\pm}_{\rm eff}$. These two problems have now been corrected.

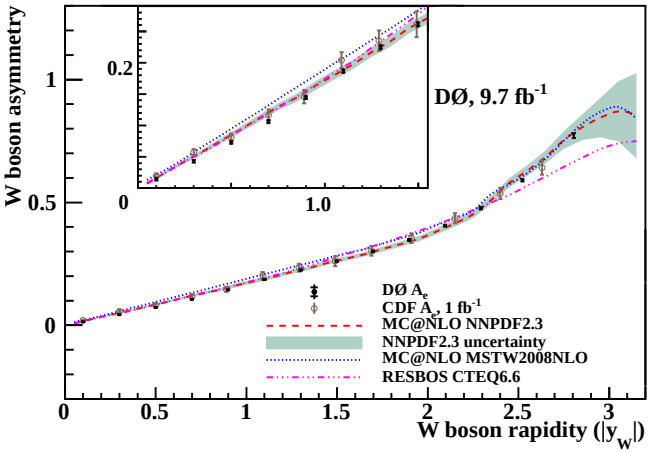

FIG. 1: (color online). Measured W boson charge asymmetry, after CP-folding, compared to predictions and the CDF 1 fb^{-1} result. The points show the measured asymmetry, with the horizontal bars delineating the statistical uncertainty component and the vertical lines showing the total uncertainty. The central value and uncertainty from MC@NLO [26] using the NNPDF2.3 [30] PDF sets and the predictions from RESBOS [23] using the CTEQ6.6 [21] central PDF set and MC@NLO using the MSTW2008NLO [32] central PDF set are also shown. The inset focuses on the y_W region from 0 to 1.5.

The corrected W boson charge asymmetry values measured using the updated efficiency correction [2] are given in Table I. These revised measurements, together with those from the CDF Collaboration [12] are shown in Fig. 1. The asymmetry values have changed relative to those in the original publication by $< 2\%$, with smaller asymmetry values for $|y_W| < 0.6$ and larger asymmetry values for $0.8 < |y_W| < 2.4$, compared to the published result [1].

*with visitors from [a]Augustana College, Sioux Falls, SD, USA, [b]The University of Liverpool, Liverpool, UK, [c]DESY, Hamburg, Germany, [d]Universidad Michoacana de San Nicolas de Hidalgo, Morelia, Mexico [e]SLAC, Menlo Park, CA, USA, [f]University College London, London, UK, [g]Centro de Investigacion en Computacion - IPN, Mexico City, Mexico, [h]Universidade Estadual Paulista, São Paulo, Brazil, [i]Karlsruher Institut für Technologie (KIT) - Steinbuch Centre for Computing (SCC), D-76128 Karlsrue, Germany, [j]Office of Science, U.S. Department of Energy, Washington, D.C. 20585, USA and [k]American Association for the Advancement of Science, Washington, D.C. 20005, USA.

[1] V. M. Abazov *et al.* (D0 Collaboration), Phys. Rev. Lett **112**, 151803 (2014).
[2] V. M. Abazov *et al.* (D0 Collaboration), arXiv: 1412.2862 (2014), submitted to Phys. Rev. D.
[3] T. Aaltonen *et al.* (CDF Collaboration), Phys. Rev. Lett. **102**, 181801 (2009).
[4] S. Frixione and B. R. Webber, J. High Energy Phys. **06**,

TABLE I: CP-folded W boson charge asymmetry for data and predictions from MC@NLO using the NNPDF2.3 PDFs tabulated in percent (%) for each $|y_W|$ bin. The $\langle|y_W|\rangle$ is calculated as the cross section weighted average of y_W in each bin from RESBOS with PHOTOS [31]. For data, the first uncertainty is statistical and the second is systematic. The uncertainties on the prediction come from both the PDF uncertainties and α_s uncertainties.

Bin index	$\lvert y_W\rvert$	$\langle\lvert y_W\rvert\rangle$	Data	Prediction
1	0.0–0.2	0.10	$1.39 \pm 0.17 \pm 0.12$	1.61 ± 0.19
2	0.2–0.4	0.30	$4.28 \pm 0.18 \pm 0.19$	5.06 ± 0.33
3	0.4–0.6	0.50	$7.28 \pm 0.19 \pm 0.27$	8.50 ± 0.41
4	0.6–0.8	0.70	$10.59 \pm 0.20 \pm 0.30$	12.05 ± 0.53
5	0.8–1.0	0.90	$14.45 \pm 0.21 \pm 0.32$	15.36 ± 0.66
6	1.0–1.2	1.10	$18.63 \pm 0.22 \pm 0.39$	18.86 ± 0.74
7	1.2–1.4	1.30	$22.50 \pm 0.24 \pm 0.44$	22.52 ± 0.80
8	1.4–1.6	1.50	$26.12 \pm 0.27 \pm 0.42$	26.30 ± 0.85
9	1.6–1.8	1.70	$30.06 \pm 0.31 \pm 0.44$	29.89 ± 0.92
10	1.8–2.0	1.90	$34.73 \pm 0.35 \pm 0.49$	34.04 ± 1.08
11	2.0–2.2	2.10	$40.59 \pm 0.40 \pm 0.54$	39.77 ± 1.31
12	2.2–2.4	2.29	$47.65 \pm 0.44 \pm 0.56$	47.73 ± 1.62
13	2.4–2.7	2.52	$59.04 \pm 0.46 \pm 0.60$	61.81 ± 1.74
14	2.7–3.2	2.81	$77.24 \pm 0.93 \pm 0.66$	78.05 ± 4.36

029 (2002).
[5] R. D. Ball *et al.*, Nucl. Phys. **B867**, 244 (2013).
[6] C. Balazs and C. P. Yuan, Phys. Rev. D **56**, 5558 (1997).
[7] J. Pumplin, D. R. Stump, J. Huston, H.-L. Lai, P. Nadolsky, and W.-K. Tung, J. High Energy Phys. **07** 012 (2002); D. Stump, J. Huston, J. Pumplin, W.-K Tung, H.-L. Lai, S. Kuhlmann, and J. F. Owens, J. High Energy Phys. **10**, 046 (2003).
[8] A.D. Martin, W. J. Stirling, R. S. Thorne, and G. Watt, Eur. Phys. J. C **63**, 189 (2009).
[9] P. Golonka and Z. Wąs, Eur. Phys. J. C **45**, 97 (2006).

Measurement of the W Boson Production Charge Asymmetry in $p\bar{p} \to W + X \to e\nu + X$ Events at $\sqrt{s} = 1.96$ TeV

We present a measurement of the W boson production charge asymmetry in $p\bar{p} \to W + X \to e\nu + X$ events at a center of mass energy of 1.96 TeV, using 9.7 fb^{-1} of integrated luminosity collected with the D0 detector at the Fermilab Tevatron Collider. The neutrino longitudinal momentum is determined by using a neutrino weighting method, and the asymmetry is measured as a function of the W boson rapidity. The measurement extends over wider electron pseudorapidity region than previous results and is the most precise to date, allowing for precise determination of proton parton distribution functions in global fits.

(Dated: December 10, 2013)

At the Fermilab Tevatron Collider, production of $W^{\pm}$ bosons is dominated by the annihilation of valence quarks in the proton (u, d) and antiproton ($\bar{d}$, $\bar{u}$). The primary modes of production are $u + \bar{d} \to W^+$ and $\bar{u} + d \to W^-$. In the proton and antiproton, the u ($\bar{u}$) quark generally carries more momentum than the $\bar{d}$ (d) quark; thus, W^+ bosons are boosted in the proton direction and W^- bosons in the antiproton direction [1–3]. The difference between u and d quark parton distribution functions (PDFs) results in a charge asymmetry in the W boson rapidity (y_W), defined as

$$A(y_W) = \frac{d\sigma_{W^+}/dy_W - d\sigma_{W^-}/dy_W}{d\sigma_{W^+}/dy_W + d\sigma_{W^-}/dy_W}. \quad (1)$$

Here, $d\sigma_{W^{\pm}}/dy_W$ is the differential cross section for $W^{\pm}$ boson production, and y_W is the $W^{\pm}$ boson rapidity, defined as

$$y_W = \frac{1}{2} \ln \frac{E + p_z}{E - p_z}, \quad (2)$$

where E and p_z are the energy and the longitudinal momentum, respectively, of the W boson, with the z axis along the proton beam direction.

Previously published results include both lepton (from the W boson decay) and W boson charge asymmetries. The lepton charge asymmetry arises from the convolution of the W boson asymmetry and the $V-A$ structure of the W boson decay. This implies that leptons at a specific rapidity originate from a wide range of W rapidities, and therefore from a wide range of parton x values (where x is the fraction of momentum of the proton carried by the parton), diluting the impact of these asymmetries when determining PDFs. The lepton charge asymmetry in W boson decays has been measured by the CDF [4–6] and D0 [7, 8] Collaborations. The latest lepton charge asymmetry measurement from the D0 Collaboration was performed in the $W \to \mu\nu$ muon channel by using data corresponding to 7.3 fb^{-1} of integrated luminosity [9]. The lepton charge asymmetry has also been measured at the Large Hadron Collider (LHC) in pp collisions by the ATLAS [10] and CMS [11] Collaborations by using integrated luminosities of 0.03 and 0.84 fb^{-1}, respectively. A direct measurement of the W boson charge asymmetry was performed by using 1 fb^{-1} of integrated luminosity by the CDF [12] Collaboration.

The analysis presented in this Letter uses the $W \to e\nu$ decay mode and employs the neutrino weighting method [13]. In addition, this W boson charge asymmetry analysis uses 10 times more integrated luminosity and covers much larger rapidity range than the previous CDF result [12]. We use data corresponding to 9.7 fb^{-1} of integrated luminosity [14] collected with the D0 detector [15, 16] between April 2002 and September 2011. By extending the pseudorapidity coverage, we can provide information about the PDFs for a broader range of x ($0.002 < x < 0.99$ for electron pseudorapidity $|\eta^e| < 3.2$ [17]) at $Q^2 \approx M_W^2$, where Q^2 is the squared momentum scale for the parton interactions and M_W is the W boson mass. The W boson charge asymmetry result places stringent constraints on the PDFs of valence quarks, which in turn will significantly reduce the uncertainty on the measurements of M_W and on other measurements at the Tevatron and LHC.

The D0 detector [15, 16] comprises a central tracking system, a calorimeter, and a muon system. The central tracking system consists of a silicon microstrip tracker and a scintillating fiber tracker (CFT). The CFT provides coverage for charged particles at detector pseudorapidities of $|\eta_{\rm det}| < 1.7$. Three liquid argon and uranium calorimeters provide coverage of $|\eta_{\rm det}| < 3.5$ for electrons: the central calorimeter (CC) up to $|\eta_{\rm det}| < 1.1$ and two end calorimeters (EC) in the range $1.5 < |\eta_{\rm det}| < 3.5$. Gaps between the cryostats create an inefficient electron detection region between $1.1 < |\eta_{\rm det}| < 1.5$ that is excluded from the analysis. Each calorimeter consists of an inner electromagnetic (EM) section, followed by hadronic sections.

Events used in this analysis were collected with a set of calorimeter-based single-electron triggers. To select $W \to e\nu$ events, we require one EM shower with transverse energy will respect to the beam $25 < E_T < 100$ GeV measured in the calorimeter, accompanied by large missing transverse energy of $\not\!\!E_T > 25$ GeV. $\not\!\!E_T$ is estimated by the vector sum of the transverse components of the energy deposited in the calorimeter (u_T) and the electron E_T. An isolation requirement is imposed on the electron candidate, which is also required to have a significant fraction of its energy deposited in the EM calorimeter, compared to that deposited in the hadron calorimeter. Candidates in the CC must be in the range $|\eta_{\rm det}| < 1.1$, and those in the EC must be within $1.5 < |\eta_{\rm det}| < 3.2$, to allow a precise measurement of elec-

tron energy. The shower shape [18] must be consistent with that expected for an electron, and the candidate is required to be spatially matched to a reconstructed track. Because the CFT detector does not cover the entire $\eta_{\rm det}$ region used in the analysis, electron selection criteria are separately defined in four categories: CC electrons with full CFT coverage, EC electrons with full CFT coverage, EC electrons with partial CFT coverage, and EC electrons without CFT coverage. Events are further required to have the reconstructed $p\bar{p}$ interaction vertex located within 40 cm of the detector center along the z axis, a reconstructed W boson transverse mass (M_T) between 50 and 130 GeV, where $M_T = \sqrt{2E_T \not\!\!E_T (1-\cos\Delta\phi)}$, and $\Delta\phi$ is the azimuthal angle between the electron and $\not\!\!E_T$, u_T less than 60 GeV, and SET less than 250 or 500 GeV depending on the data collection period, where SET is the scalar sum of all transverse energies measured by the calorimeter except those energies associated with electrons or with potential noise, reflecting the total activity in the event.

After applying the selection criteria described above, we retain 6 083 198 W boson candidates. Of these, 4 466 735 are events with the electron in the CC region and 1 616 463 with the electron in the EC region. We have checked that the asymmetry results for $y_W > 0$ are consistent with those for $y_W < 0$, so we assume CP invariance—*i.e.*, $A(y_W)$ is equivalent to $-A(-y_W)$—and fold the data appropriately to increase the statistics in each y_W bin. The forward-backward charge asymmetries are measured in 14 bins of y_W in the range $|y_W| < 3.2$. The bin widths are chosen by considering the sample size and the detector geometry to ensure that high $|y_W|$ bins retain sufficient statistics.

Mismeasurement of the charge sign of the electron may result in a dilution of the W boson charge asymmetry. We measure the charge misidentification rate with $Z \to ee$ events, using a "tag-and-probe" method [19]. The tag electron must satisfy tight selection criteria to ensure its charge is determined correctly. The charge misidentification rate varies from $(0.18 \pm 0.01)\%$ at $|\eta^e| = 0$ to $(9.6 \pm 0.9)\%$ at $|\eta^e| = 3.0$, where tracking momentum resolution is poor. The direction of the D0 solenoid magnetic fields was reversed during data taking every two weeks on average, significantly reducing the charged particle reconstruction asymmetry in the detector; thus, the charge misidentification rates of electrons and positrons are consistent for different magnet polarities. At $|\eta^e| = 3.0$, the charge misidentification rates are $(9.4 \pm 1.3)\%$ for electrons and $(9.8 \pm 1.3)\%$ for positrons and are also consistent with each other at other $|\eta^e|$ values.

Monte Carlo (MC) samples for the $W \to e\nu$ process are generated by using the PYTHIA [20] event generator with CTEQ6L1 PDFs [21], followed by a GEANT-based simulation [22] of the D0 detector. This simulation is then corrected for higher-order effects not included in PYTHIA. The MC events are reweighted at the generator level in two dimensions (W boson transverse momentum, p_T^W, and y_W) to match RESBOS [23] predictions. To improve the accuracy of the MC detector simulation, further corrections are applied to the MC simulations including electron energy scale and resolution, recoil system scale and resolution, selection efficiencies, trigger efficiencies, instantaneous luminosity and SET, charge misidentification, and relative efficiency for identification of positrons and electrons ($K^{\pm}_{\rm eff}$). These corrections are derived by comparing the $Z \to ee$ data and PYTHIA MC distributions. Because of imperfections in the modeling of the tracking detector, differences between the efficiency for electrons and positrons vary from 0.0% at $|\eta^e| = 0$ to 1% at $|\eta^e| = 3.0$.

The dominant source of background originates from multijet events, with one jet misreconstructed as an electron and with significant $\not\!\!E_T$ due to the mismeasurement of the jet energy. Smaller background contributions arise from other standard model (SM) processes and are estimated by using PYTHIA MC samples normalized to the highest order available cross sections [24]. These include $W \to \tau\nu$ events where the tau decays to an electron and neutrinos, $Z \to ee$ events where one of the electrons is not identified, and $Z \to \tau\tau$ events with one tau decaying to an electron and the other not identified. The multijet background is estimated by using collider data by fitting the M_T distribution in the region 50-130 GeV (after other SM backgrounds have been subtracted) to the sum of the shape predicted by the $W \to e\nu$ signal MC sample and the shape obtained from a multijet-enriched data sample. The multijet-enriched sample is selected by reversing the shower shape requirement on the electron candidates. The background contributions are determined as a function of y_W, and average contributions are 4.0% multijet events, 2.6% $Z \to ee$, 2.2% $W \to \tau\nu$, and 0.2% $Z \to \tau\tau$.

In the determination of the longitudinal momentum of the neutrino (p_z^ν) [13], M_W is fixed to the world average value of 80.385 GeV [25]. The mass-energy relation constraint using the energy and momentum of the neutrino and electron,

$$M_W^2 = (E_e + E_\nu)^2 - (\vec{P}_e + \vec{P}_\nu)^2, \qquad (3)$$

implies that there are two solutions in p_z^ν. The twofold ambiguity can be partly resolved on a statistical basis from the known $V-A$ decay distribution by using the decay angle between the electron and the proton (θ^*) and from the W^+ and W^- production cross sections as a function of y_W. As expected, many off-shell W boson decays do not satisfy the M_W^2 constraint. In this case, we obtain complex values for the p_z^ν, assume that the neutrino transverse momentum (p_T^ν) is misreconstructed, and therefore scale $\not\!\!E_T$ to the value for which the imaginary part equals zero. This new $\not\!\!E_T$ value is then used to determine p_T^ν and therefore y_W. To obtain the W boson

rapidity distributions, we assign different probabilities to the two p_z^ν solutions. This probability is related to the quark and antiquark $W^\pm$ boson production by

$$P_\pm\left(\cos\theta^*, y_W, p_T^W\right) = \left(1 \mp \cos\theta^*\right)^2 + Q\left(y_W, p_T^W\right)\left(1 \pm \cos\theta^*\right)^2, \quad (4)$$

where $P_\pm\left(\cos\theta^*, y_W, p_T^W\right)$ is the probability for W boson production with a particular $\cos\theta^*$, y_W, and p_T^W. The first term in Eq. (4) represents the contribution from annihilation with two quarks, and the second term the contribution from annihilation with at least one antiquark. The ratio $Q\left(y_W, p_T^W\right)$ between quark and antiquark W boson production is a function of W boson rapidity and transverse momentum. At the Tevatron, the W boson production contribution from the antiquark and gluons is $\sim 10\%$.

Understanding the antiquark contribution is important for the asymmetry measurement, because W bosons produced by antiquarks have opposite polarization from those produced by quarks. The ratio of antiquark to quark W boson production is determined by the angular distribution of $W \to e\nu$ decays. We use the prediction of the fractions of antiquark to quark contributions from MC@NLO [26], using the CTEQ6.6 PDF set, and parametrize the angular distributions as functions of y_W and p_T^W, using an empirical function to fit the ratio.

We use both $P_\pm$ and the differential cross section $d\sigma_W^\pm/dy_W$ to define weights as in Eq. (5). The W boson production cross section decreases in the forward region due to the scarcity of high-x quarks, and so solutions leading to a central W production are weighted more heavily than forward W solutions. The weight factors w_i for W^+ and W^- are

$$w_i^\pm = \frac{P_\pm\left(\cos\theta_i^*, y_i, p_T^W\right) d\sigma^\pm\left(y_i\right)/dy_W}{\sum_i P_\pm\left(\cos\theta_i^*, y_i, p_T^W\right) d\sigma^\pm\left(y_i\right)/dy_W}, \quad (5)$$

where $i = 1, 2$ are the two solutions. We use the predicted differential cross section $d\sigma_W^\pm/dy_W$ at next-to-next-to-leading order [27] as input when calculating the weight factors for each neutrino p_z^ν solution. We iterate by updating values of $d\sigma_W^\pm/dy_W$ to those obtained by using the weight factor. This procedure converges after three or four iterations.

To measure the W boson charge asymmetry, we apply unfolding corrections to the measured W^+ and W^- distributions to correct detection effects. The matrix inversion method [28] is used to correct for event migration effects. First, the product of acceptance and efficiency is applied to each bin to correct for the event selection effects, and the $K_{\rm eff}^\pm$ correction is used to equalize the efficiency response between electrons and positrons. The migration matrices are obtained by using the number of events in both the generator level y_W bin j and the reconstruction level y_W bin i, divided by the number of events in the reconstruction level y_W bin i. The migration matrices provide information about the relation between events selected at reconstruction level and the original events at generator level and are used to correct the data for detector resolution effects. The procedure is validated by using events generated with MC@NLO, where we find good agreement between the unfolded and the generated W boson charge asymmetry.

The primary systematic uncertainties on asymmetry come from the unfolding procedure including the uncertainties from the event migration correction, the acceptance and efficiency correction, and the PDF inputs (fractional uncertainty, $[1.1\text{–}5.0]\times10^{-3}$). To estimate the uncertainty from the PDF inputs, we determine the $Q\left(y_W, p_T^W\right)$ correction with 45 CTEQ6.6 PDF sets, perform the measurement with different $Q\left(y_W, p_T^W\right)$ [29], and extract the uncertainty for each y_W bin using the prescription described in Ref. [21]. Other systematic uncertainties arise from the modeling of the p_T^W distribution and the final state radiation modeling ($[0.1\text{–}2.4]\times10^{-4}$), electron identification corrections ($[0.1\text{–}0.7]\times10^{-3}$), electron energy modeling ($[0.1\text{–}0.5]\times10^{-3}$), hadronic recoil modeling ($[0.1\text{–}0.8]\times10^{-3}$), background modeling ($[0.1\text{–}1.0]\times10^{-3}$), MC modeling imperfections ($[0.2\text{–}2.6]\times10^{-3}$), electron charge misidentification ($[0.1\text{–}2.0]\times10^{-3}$), and the relative efficiency for positrons and electrons ($K_{\rm eff}^\pm$) ($[0.1\text{–}0.6]\times10^{-3}$).

Figure 2 shows the measured values of the W boson asymmetry together with the result from CDF [12]. The data are compared to the MC@NLO prediction with the NNPDF2.3 [30] PDF set, next-to-leading order RESBOS prediction with PHOTOS [31] using the CTEQ6.6 central PDF set, and MC@NLO using MSTW2008NLO [32] central PDF set. In the predictions, we require both the electron and neutrino transverse momentum to be above 25 GeV and merge the radiated photons into the electron if they fall within a cone of radius $\Delta R = \sqrt{(\Delta\phi)^2 + (\Delta\eta)^2} < 0.3$. There is agreement between the data and predictions, although the predictions are systematically higher than the data by ~ 1 standard deviation in all measurements for $|y_W|$ between 0.1 and 1. Values of the asymmetry in bins of y_W, average bin positions, and predictions are shown in Table II. The experimental uncertainties are substantially smaller than the uncertainties from the NNPDF2.3 PDF sets in all y_W bins, demonstrating the importance of this analysis to improve PDFs. Table III lists the correlations between central values in different y_W bins that are introduced by the ambiguity in p_z^ν. The correlation coefficients of systematic uncertainties between different y_W are negligible.

In summary, we have measured the W boson charge asymmetry in $p\bar{p} \to W \to e\nu$ events by using data corresponding to 9.7 fb^{-1} of integrated luminosity collected

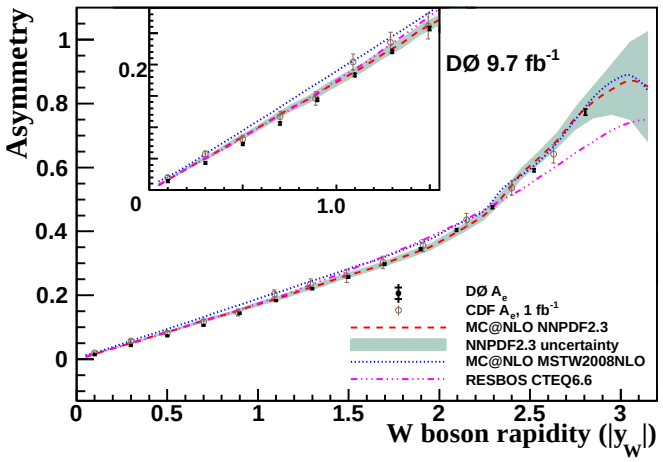

FIG. 2: (color online). Measured W boson charge asymmetry, after CP folding, compared to predictions and the CDF 1 fb^{-1} result. The points show the measured asymmetry, with the horizontal bars delineating the statistical uncertainty component and the vertical lines showing the total uncertainty. The central value and uncertainty from MC@NLO using NNPDF2.3 PDF sets and the prediction from RESBOS using the CTEQ6.6 central PDF set, MC@NLO using the MSTW2008NLO central PDF set are also shown. The inset focuses on the y_W region from 0 to 1.5.

TABLE II: CP-folded W charge asymmetry for data and predictions from MC@NLO using NNPDF2.3 PDFs tabulated in percent (%) for each $|y_W|$ bin. The $\langle|y_W|\rangle$ is calculated as the cross section weighted average of y_W in each bin from RESBOS with PHOTOS. For data, the first uncertainty is statistical and the second is systematic. The uncertainties on the prediction come from both the PDF uncertainties and α_s uncertainties.

Bin index	$\lvert y_W\rvert$	$\langle\lvert y_W\rvert\rangle$	Data	Prediction
1	0.0–0.2	0.10	$1.40 \pm 0.17 \pm 0.12$	1.61 ± 0.19
2	0.2–0.4	0.30	$4.32 \pm 0.18 \pm 0.19$	5.06 ± 0.33
3	0.4–0.6	0.50	$7.33 \pm 0.19 \pm 0.27$	8.50 ± 0.41
4	0.6–0.8	0.70	$10.59 \pm 0.20 \pm 0.32$	12.05 ± 0.53
5	0.8–1.0	0.90	$14.36 \pm 0.21 \pm 0.34$	15.36 ± 0.66
6	1.0–1.2	1.10	$18.32 \pm 0.22 \pm 0.37$	18.86 ± 0.74
7	1.2–1.4	1.30	$22.06 \pm 0.24 \pm 0.39$	22.52 ± 0.80
8	1.4–1.6	1.50	$25.74 \pm 0.27 \pm 0.36$	26.30 ± 0.85
9	1.6–1.8	1.70	$29.75 \pm 0.31 \pm 0.34$	29.89 ± 0.92
10	1.8–2.0	1.90	$34.46 \pm 0.35 \pm 0.38$	34.04 ± 1.08
11	2.0–2.2	2.10	$40.42 \pm 0.40 \pm 0.43$	39.77 ± 1.31
12	2.2–2.4	2.29	$47.55 \pm 0.44 \pm 0.43$	47.73 ± 1.62
13	2.4–2.7	2.52	$59.10 \pm 0.46 \pm 0.44$	61.81 ± 1.74
14	2.7–3.2	2.81	$77.33 \pm 0.93 \pm 0.56$	78.05 ± 4.36

by the D0 experiment at $\sqrt{s} = 1.96$ TeV. By using the neutrino weighting method, the most precise direct measurement of the W boson charge asymmetry to date is obtained. With coverage extended to $|\eta^e| = 3.2$, this measurement can be used to improve the precision and accuracy of next-generation PDF sets; in particular, it provides more accurate information for PDFs at high x, compared with measurements of the lepton charge asymmetry, which is crucial for many beyond SM searches.

ACKNOWLEDGEMENTS

We thank the staffs at Fermilab and collaborating institutions and acknowledge support from the DOE and NSF (USA); CEA and CNRS/IN2P3 (France); MON, NRC KI, and RFBR (Russia); CNPq, FAPERJ, FAPESP, and FUNDUNESP (Brazil); DAE and DST (India); Colciencias (Colombia); CONACyT (Mexico); NRF (Korea); FOM (The Netherlands); STFC and the Royal Society (United Kingdom); MSMT and GACR (Czech Republic); BMBF and DFG (Germany); SFI (Ireland); The Swedish Research Council (Sweden); and CAS and CNSF (China).

[1] E.L. Berger, F. Halzen, C.S. Kim and S. Willenbrock, Phys. Rev. D **40**, 83 (1989).
[2] A.D. Martin, R.G. Roberts, and W.J. Stirling, Mod. Phys. Lett. A **4**, 1135 (1989).
[3] H.-L. Lai, J. Boots, J. Huston, J. G. Morfin, J. F. Owens, J. W. Qiu, W.-K. Tung, and H. Weerts, Phys. Rev. D **51**, 4763 (1995).
[4] F. Abe *et al.* (CDF Collaboration), Phys. Rev. Lett. **74**, 850 (1995).
[5] F. Abe *et al.* (CDF Collaboration), Phys. Rev. Lett. **81**, 5754 (1998).
[6] D. Acosta *et al.* (CDF Collaboration), Phys. Rev. D **71**, 051104 (2005).
[7] V. M. Abazov *et al.* (D0 Collaboration), Phys. Rev. D **77**, 011106 (2008).
[8] V. M. Abazov *et al.* (D0 Collaboration), Phys. Rev. Lett. **101**, 211801 (2008).
[9] V. M. Abazov *et al.* (D0 Collaboration), Phys. Rev. D **88**, 091102(R) (2013).
[10] G. Aad *et al.* (ATLAS Collaboration), Phys. Lett. B **701**, 31 (2011).
[11] S. Chatrchyan *et al.* (CMS Collaboration), Phys. Rev. Lett. **109**, 111806 (2012).
[12] T. Aaltonen *et al.* (CDF Collaboration), Phys. Rev. Lett. **102**, 181801 (2009).
[13] A. Bodek, Y. Chung, B.-Y. Han, K. McFarland, and E. Halkiadakis, Phys. Rev. D **77**, 111301(R) (2008).
[14] T. Andeen *et al.*, Report No. FERMILAB-TM-2365, 2007.
[15] S. Abachi *et al.* (D0 Collaboration), Nucl. Instrum. Methods Phys. Res., Sect. A **338**, 185 (1994).

TABLE III: Correlation coefficients between central values of asymmetry in different $|y_W|$ bins.

$\lvert y_W\rvert$ bin	1	2	3	4	5	6	7	8	9	10	11	12	13	14
1	1.00	0.84	0.57	0.38	0.29	0.25	0.21	0.16	0.10	0.06	0.04	0.03	0.02	0.01
2		1.00	0.85	0.58	0.39	0.29	0.24	0.16	0.11	0.07	0.04	0.04	0.03	0.02
3			1.00	0.85	0.58	0.38	0.26	0.16	0.10	0.06	0.05	0.06	0.05	0.03
4				1.00	0.83	0.52	0.29	0.16	0.09	0.07	0.08	0.10	0.09	0.06
5					1.00	0.78	0.42	0.19	0.11	0.10	0.13	0.15	0.14	0.10
6						1.00	0.74	0.37	0.22	0.19	0.22	0.22	0.20	0.15
7							1.00	0.76	0.50	0.38	0.34	0.31	0.29	0.21
8								1.00	0.84	0.62	0.47	0.38	0.34	0.27
9									1.00	0.87	0.65	0.48	0.40	0.31
10										1.00	0.89	0.67	0.51	0.36
11											1.00	0.89	0.66	0.41
12												1.00	0.86	0.45
13													1.00	0.50
14														1.00

[16] V. M. Abazov *et al.* (D0 Collaboration), Nucl. Instrum. Methods Phys. Res., Sect. A **565**, 463 (2006).

[17] D0 uses a cylindrical coordinate system with the z axis along the beam axis in the proton direction. Angles θ and ϕ are the polar and azimuthal angles, respectively. Pseudorapidity is defined as $\eta = -\ln[\tan(\theta/2)]$ where θ is measured with respect to the interaction vertex. In the massless limit, η is equivalent to the rapidity $y = (1/2)\ln[(E+p_z)/(E-p_z)]$, and $\eta_{\rm det}$ is the pseudorapidity measured with respect to the center of the detector.

[18] S. Abachi *et al.* (D0 Collaboration), Nucl. Instrum. Meth. Phys. Res., Sect. A **324**, 53 (1993).

[19] V. Abazov *et al.* (D0 Collaboration), Phys. Rev. D **76**, 012003 (2007).

[20] T. Sjöstrand, P. Edén, C. Feriberg, L. Lönnblad, G. Miu, S. Mrenna, and E. Norrbin, Comput. Phys. Commun. **135**, 238 (2001). PYTHIA version v6.323 is used.

[21] J. Pumplin, D. R. Stump, J. Huston, H.-L. Lai, P. Nadolsky, and W.-K. Tung, J. High Energy Phys. 07 (2002) 012; D. Stump, J. Huston, J. Pumplin, W.-K Tung, H.-L. Lai, S. Kuhlmann, and J. F. Ownes, J. High Energy Phys. 10 (2003) 046.

[22] R. Brun and F. Carminati, CERN Program Library Long Writeup W5013, 1993 (unpublished).

[23] C. Balazs and C. P. Yuan, Phys. Rev. D **56**, 5558 (1997).

[24] R. Hamberg, W.L. van Neerven, and T. Matsuura, Nucl. Phys. B **359**, 343 (1991).

[25] J. Beringer *et al.* (Particle Data Group), Phys. Rev. D **86**, 010001 (2012).

[26] S. Frixione and B. R. Webber, J. High Energy Phys. 06 (2002) 029.

[27] C. Anastasiou, L. Dixon, K. Melnikov, and F. Petriello, Phys. Rev. D **69**, 094008 (2004).

[28] G. L. Marchuk, *Methods of Numerical Mathematics* (Springer, Berlin, 1975).

[29] See Supplemental Material at http://link.aps.org/supplemental/10.1103/PhysRevLett.112.151803 for the measured W boson charge asymmetry central values using 45 CTEQ6.6 different PDF sets as input.

[30] R. D. Ball *et al.*, Nucl. Phys. B **867**, 244 (2013).

[31] P. Golonka and Z. Wąs, Eur. Phys. J. C **45**, 97 (2006).

[32] A.D. Martin, W. J. Stirling, R. S. Thorne, and G. Watt, Eur. Phys. J. C **63**, 189 (2009).